Journal of Quantitative Spectroscopy & Radiative Transfer 276 (2021) 107943

Contents lists available at ScienceDirect

Journal of Quantitative Spectroscopy & Radiative Transfer

journal homepage: www.elsevier.com/locate/jqsrt

Branching fraction measurements of arsenic $4p^25s$-$4p^3$ transitions

U. Berzins [a,b,*], A. Ubelis [a,b], A. Bziskjans [a,b]

[a] Institute of Atomic Physics and Spectroscopy, University of Latvia, Jelgavas street 3, Riga LV-1004, Latvia
[b] National Scientific Platform FOTONIKA-LV, University of Latvia LV-1586, Riga, Latvia

ARTICLE INFO

Article history:
Received 6 June 2021
Revised 12 September 2021
Accepted 15 September 2021
Available online 20 September 2021

ABSTRACT

Transition lines of neutral arsenic atom (As I) have been observed in the spectra of stellar and sub-stellar objects. Accurate and reliable data of oscillator strengths of those transitions allow differentiating between different evolution models of those objects. We have measured branching fractions for As I ($4p^25s$-$4p^3$) transition lines in 180–310 nm spectral range with higher increased accuracy using light source powered by inductively coupled radio frequency plasma (RF-ICP) source – not earlier applied in studies of atomic arsenic. The measurements were performed for 7 excited states of As I and compared with data from the literature. We combined them with the selected lifetime values reported in the literature. The transition probabilities for 26 spectral lines are obtained and compared with other experimental and theoretical data from literature. The absorption oscillator strengths for two As I ($4p^25s$-$4p^3$) resonance transitions (197.3 nm, $f = 0.127$, and 193.8 nm $f = 0.059$) are also reported.

1. Introduction

The spectra from neutral atoms of various elements have been observed for different stellar and sub-stellar objects. Spectra can be useful for the prediction of the galactic chemical evolution. Such a prediction heavily relies on the accuracy of the oscillator strength measurement data of the observed transitions, since inaccurate atomic data leads to uncertainties in differentiating between different evolution models. Among the elements suitable for improved laboratory study is arsenic, rarely observed but important for understanding the production of light neutron-capture elements.

The absorption lines of atomic arsenic (As I) were firstly reported in studies of binary star *Chi Lupi* during the first mission of Hubble Space Telescope launched into low Earth orbit in 1990 [1]. Later, As I lines were detected in a couple of metal poor stars [2–4] and in interstellar space [5]. The abundance of this element was calculated by analysing the atomic absorption lines. The oscillator strengths of observed atomic transitions are critical for accurate determination of the quantitative parameters required for the chosen evolution models. Currently, the theoretically determined oscillator strengths are available for quite a large number of As I lines. However, up to now only the results of two experiments have been reported [6,7], which have been obtained from one set of branching fraction measurements in hollow cathode discharge lamp [6]. In order to find and rule out possible systematic errors that could occur using one particular method and experimental equipment, additional measurements with other equipment with different experimental approaches is needed. A wider range of experimental data will also give more confidence in the tests of previous theoretical calculations [8,9].

The uncertainty in determination of branching fraction depends on measurement data error, the calibration error of the spectral response of experimental system, and from the impact of self-absorption in resonance lines corresponding to transitions from the excited state to the ground state. In the present work, we used an experimental setup containing previously unconsidered major elements [6]: the RF-ICP powered arsenic spectral line source, monochromator, detector and calibration sources. The lifetimes of As I excited states from other studies [7,10] were used to convert the measured branching fractions to the transition probabilities or Einstein coefficients. They have been measured by using the beam foil method [10] and by short pulse laser induced fluorescence detection [7].

2. Experimental arrangements

Lifetimes, branching fractions, transition probabilities and oscillator strengths are interconnected parameters for each specific element of the periodic table. The branching ratios or branching fractions (b_{ul}) are the relative transition probabilities from the upper level "u" to all lower energy levels "l" allowed by selection rules.

* Corresponding author.
E-mail address: uberz@lu.lv (U. Berzins).

https://doi.org/10.1016/j.jqsrt.2021.107943

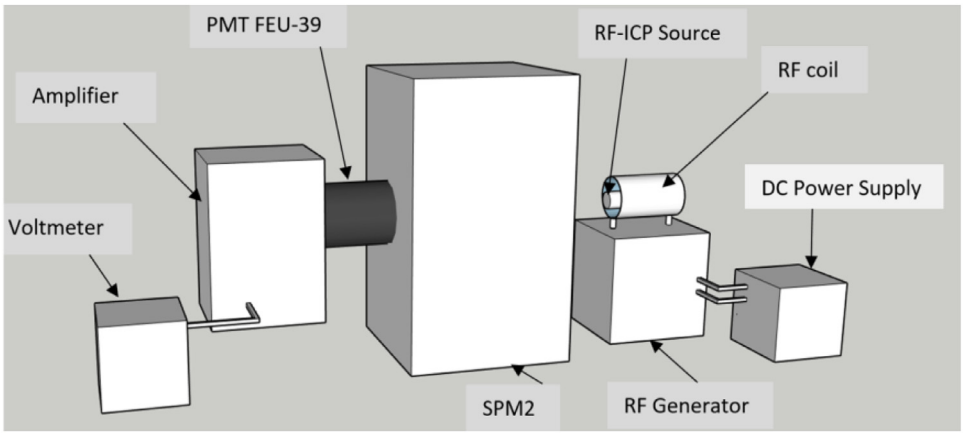

Fig. 1. Schematic of the experimental set-up.

The sum of them is normalized to one:

$$\Sigma_l b_{ul} = 1 \quad (1)$$

The absolute values of transition probabilities or Einstein coefficients are determined by normalizing them to the inverse radiative lifetime (τ_u) of corresponding excited state:

$$\Sigma_l A_{ul} = 1/\tau_u \quad (2)$$

For abundance determination the oscillator strengths values (f_{lu}) are used. They can be calculated from transition probability (A_{ul}) by using the following expression:

$$f_{lu} = 1.5 \times (g_u/g_l)\lambda^2 A_{ul} \times 10^{-18}, \quad (3)$$

where λ is the wavelength in nanometres and gu and gl are the statistical weights for corresponding levels.

The uncertainty in determining transition probabilities values depends on errors in both: the lifetime and branching fraction values. The relationship between the above values, as well as a detailed description for the calculation of measurement errors, are discussed in [11], in relation to oscillator strengths measurement method for applications in astrophysics.

In our measurements, the method described in previous studies of selenium [12] and tellurium [13] atoms was used. The As I emission lines were obtained from the laboratory-made light source powered RF-ICP generator [14]. Light sources - two sealed lamp bulbs - were made of high quality silica of 18 mm diameter spheres filled with As+Xe and As+Xe+KBr. In the manufacturing process, bulbs were attached to a high purity vacuum pumping system and a high purity Xe gas inlet system that ensured the filling of gasses in lamp bulbs with a precision of a few mbar. The bulb inner surfaces were repeatedly cleaned via discharge in Xe environment. Bulbs were pumped out to reach a vacuum higher than 10^{-6} torr before lamp body was filled with few micrograms of arsenic and 100 mbar of Xe. Then bulbs were sealed off from the vacuum system. In order to test the branching ratios in different discharge plasma conditions, a few micrograms of KBr was added in the second lamp. The lamp bulb was placed inside the coil of generator and the plasma discharge was powered by 54 MHz frequency of RF-ICP generator with external voltage supply (Fig. 1).

The spectral lines of As I were analysed by a double mirror high quality silica prisma monochromator SPM-2 (Carl Zeiss Jena) ensuring high resolution and high quality of spectra in the 200–300 nm range [15]. Working with a reasonably opened slit allowed the capture of very weak light-source signals. Intensities of each spectral lines were detected using photomultiplier tube PMT 39A [16] that is effective in far UV attached at the exit slit of monochromator. Photocurrent was amplified and measured using a voltmeter. The calibration of spectral response of the system was performed using a hydrogen lamp DBC-25 [17], and a deuterium lamp made and calibrated in Vavilov State Optical Institute [18]. Using the calibration curves for both above mentioned lamps we estimated the uncertainty of the detection system being below 15% in the area 190–300 nm.

3. Results

Photocurrent detected for each spectral line is directly proportional to the radiation intensity. The measurement of individual lines were performed by tuning the monochromator to the needed wavelength and by adjusting the reading on maxima. In order to exclude the influence of possible instabilities of the line source, measurements were performed for pairs of lines with common upper level. At the constant DC power supplied to the RF generator the photocurrent measurements were repeated by sequential changing from the first line to the second one. In order to investigate the influence of self-absorption, the measurements were performed at different powers in the area where intensities of spectral lines changed in the range of two orders of magnitude. After each change of DC power an intensity of a spectral line was stabilized during a few minutes before measurements were performed. The ratio of measured photocurrents "i_1"and "i_0"is transformed to the ratio of spectral line intensities I_1/I_0 by taking into account the calibration curve of the experimental setup.

It is worth noting that the influence of self-absorption was observed only at increased power for resonance lines 197.3 nm and 193.7 nm, while reabsorption was absent for other lines for the whole range of power used for feeding arsenic lamps. Branching fractions were calculated from intensity ratios I_1/I_0, at a condition where self-absorption did not take place. In order to obtain best results the intensity ratio for two lines was evaluated from more than 10 individual measurements with two lamps at different powers. The scattering of data was within 2%. Therefore, the uncertainty in the intensity ratio was dominated by the above-mentioned 15% calibration error. The ratio of branching fractions b_1/b_0 were calculated from the measured intensity ratios - the photon energies were taken as inversely proportional to wavelength of each spectral line.

$$b_1/b_0 = (I_1/I_0) \times (\lambda_0/\lambda_1), \quad (4)$$

where λ_0 and λ_1 are wavelengths for each of measured lines.

The intensity ratios were measured for several line pairs at least one time including each line from the same upper level. The branching fractions were evaluated for all transitions from the following system of equations (5) and presented in Table 1 together

Table 1
The measured branching fractions for As I ($4p^25s$-$4p^3$) lines.

Transition	λ, nm,	This experiment	Experiment [6]*	Theory		
				[8]	[9] DV	[9] DL
$^4P_{1/2}$ – $^4S^o_{3/2}$	197.262	0.94 (1)**	0.907	0.898	0.904	0.939
– $^2D^o_{3/2}$	249.294	0.057 (6)	0.0538	0.0898	0.0815	0.0552
– $^2P^o_{1/2}$	307.531	0.0016 (2)	0.0342	0.0072	0.00831	0.00208
– $^2P^o_{3/2}$	311.959	0.0024 (3)	0.0049	0.0051	0.00676	0.00330
$^4P_{3/2}$ – $^4S^o_{3/2}$	193.759	0.94 (1)	0.941	0.936	0.926	0.950
– $^2D^o_{3/2}$	243.723	0.010 (1)	0.00722	0.0063	0.00893	0.00892
– $^2D^o_{5/2}$	245.653	0.043 (5)	0.0314	0.0458	0.0488	0.0346
– $^2P^o_{1/2}$	299.098	0.00093 (10)	0.0046	0.021	0.00297	0.00132
– $^2P^o_{3/2}$	303.285	0.0039 (4)	0.015	0.0098	0.0136	0.00460
$^4P_{5/2}$ – $^4S^o_{3/2}$	189.043	0.98 (1)	0.985	*0.0213*	0.975	0.977
– $^2D^o_{3/2}$	236.304	0.00077 (15)	0.00077	*0.809*	0.00109	0.000742
– $^2D^o_{5/2}$	238.118	0.020 (2)	0.013	*0.141*	0.0236	0.0222
– $^2P^o_{3/2}$	291.882	0.00005 (1)	.	*0.028*	0.000082	0.000028
$^2P_{1/2}$ – $^4S^o_{3/2}$	188.196	0.015 (5)	0.025	*0.979*	0.0057	0.0142
– $^2D^o_{3/2}$	234.984	0.87 (4)	0.804	*0.0011*	0.757	0.816
– $^2P^o_{1/2}$	286.043	0.095 (10)	0.143	*0.019*	0.197	0.145
– $^2P^o_{3/2}$	289.870	0.017 (3)	0.0275	*0.0002*	0.0403	0.0260
$^2P_{3/2}$ – $^4S^o_{3/2}$	183.174	0.011 (3)	0.0164	0.010	0.00305	0.00984
– $^2D^o_{3/2}$	227.136	0.0051 (5)	0.00342	0.0003	0.00104	0.00157
– $^2D^o_{5/2}$	228.812	0.79 (4)	0.684	0.726	0.627	0.718
– $^2P^o_{1/2}$	274.500	0.046 (5)	0.059	0.067	0.0815	0.0679
– $^2P^o_{3/2}$	278.022	0.15(2)	0.236	0.196	0.260	0.204
$^2D_{5/2}$ – $^4S^o_{3/2}$	164.432			0.011	0.00430	0.00664
– $^2D^o_{3/2}$	199.113	0.11(2)	0.090	0.113	0.1046	0.0973
– $^2D^o_{5/2}$	200.335	0.79 (6)	0.813	0.744	0.716	0.765
– $^2P^o_{3/2}$	237.077	0.10 (1)	0.0964	0.130	0.175	0.133
$^2D_{3/2}$ – $^4S^o_{3/2}$	164.379			0.0021	0.00086	0.00171
– $^2D^o_{3/2}$	199.035	0.78 (4)	0.778	0.704	0.632	0.686
– $^2D^o_{5/2}$	200.255	0.016 (2)	0.142	0.0056	0.00921	0.0172
– $^2P^o_{1/2}$	234.402	0.061 (7)	0.0668	0.103	0.134	0.110
– $^2P^o_{3/2}$	236.966	0.14 (2)	0.141	0.186	0.225	0.186

*In [6] the term "branching ratio" is used instead of "branching fraction".
** 0.94 (1) should be read as 0.94 ± 0.01.

with the data available from literature.

$$b_0+b_1+b_2\ldots+b_n= 1$$

$$b_1/b_0= (I_1/I_0) \times (\lambda_0/\lambda_1) \quad (5)$$

$$b_n/b_0= (I_n/I_0) \times (\lambda_0/\lambda_n).$$

The relative uncertainties for the branching fractions were obtained from the errors in the intensity ratio measurements, distributed inversely proportional to the branching fraction values. Thus, the relative error is smaller for a larger branching fraction of. For example, in the case of excited state $^4P_{1/2}$, the measured ratio between the fractions of 197.262 nm line and sum for other 3 lines is 0.94/0.06. This results in a relative error for branching fraction for resonance line about 1% while for other lines it is about 15%.

Since we do not perform our measurements in vacuum, the air absorption starts to cut down the intensities of lines at λ< 200, nm. SPM 2 monochromator allows observation of resonance lines down to 183 nm, but not shorter ones. Fortunately, the transitions from $4p^25s\ ^2D - 4p^3\ ^4S^o$ states are forbidden by selection rules and the corresponding lines should not have any impact on branching fractions for other lines starting from $4p^25s\ ^2D$ excited states.

In the data set for $4p^25s\ ^4P_{1/2}$ state, we see that our measurements indicate that branching fraction for resonance line 197.3 nm is out of range of our error-bars from another experimental study [6]. We see that the transition corresponding to the 307,5 nm line is weaker in our work than in [6], and it leads to a larger branching fraction for the 193,7 nm line. Our data for this state are in good agreement with the calculated result from [9] performed by a dipole length (DL) operator.

In the data set for $4p^25s\ ^4P_{3/2}$ state we see good agreement between our results and the measurement in [6] and calculations for resonance line 193.7 nm. For other lines, our results have a strong impact for transitions down to $^2D^o$ states and weaker down to $^2P^o$ states, about the same as DL calculation. An even better agreement is found for the $4p^25s\ ^4P_{5/2}$ state between our results and the other data, if we assume that the calculated [8] data has to be taken as they are like given for $4p^25s\ ^2P_{1/2}$ state.

For the $^4P_{5/2}$ and $^2P_{1/2}$ levels, the big difference between the calculated branching fraction [8] (in italic) and the correlating experimental data is not a serious problem - if we are plotting the calculated [8] data for $^4P_{5/2}$ in a table at rows for $^2P_{1/2}$ and vice versa, we would obtain an unexpectedly good match between all the data marked in table.

In the data set for branching fractions from $4p^25s\ ^2P$ states we see that fractions for resonance lines 188.1 and 183.1 nm in our measurements are smaller than in both the other experiment and theory. One of the reasons for this could be that the calibration of our experimental system is done by continuous spectra source, but measurements are done for narrow spectral lines.

In the data set for branching fractions from $4p^25s\ ^2D$ states we see good agreement between both experimental data, they are slightly different from theoretical data but close to DL approximation.

In order to convert branching fractions to transition probabilities we need to select lifetime values from data in literature for all 7 excited states. They are presented in Table 2.

Results in Table 2 were based on lifetime measured by time-resolved laser-spectroscopy [7], but for levels $^4P_{5/2}$, $^2P_{1/2}$, $^2P_{3/2}$, $^2D_{5/2}$, $^2D_{3/2}$ the results are from calculations by the Relativistic Optimised Hartree-Fock-Slater method (Dipole Lengths approximation

Table 2
Selected lifetimes in nsec.

State	$^4P_{1/2}$	$^4P_{3/2}$	$^4P_{5/2}$	$^2P_{1/2}$	$^2P_{3/2}$	$^2D_{5/2}$	$^2D_{3/2}$
[9] DL	4.7	4.8	4.9	2.6	2.6	3.1	3.2
[10]	3.6 (4)	3.8 (4)	3.7 (4)	3.5 (4)	3.3 (3)	2.8 (3)	
[7]	4.5 (5)	4.3 (5)					
Selected	4,5	4.3	4.3	3.0	3.0	3.0	3.0

Table 3
The transition probabilities (Einstein coefficients) for As I ($4p^25s$-$4p^3$) lines.

Transition	λ, nm,	Our data	[6]	[8]	[9] DV	[9] DL
$^4P_{1/2}$ – $^4S^o_{3/2}$	197.262	209 (6)	252 (6)	108 (6)	112 (6)	199 (6)
– $^2D^o_{3/2}$	249.294	127 (5)	149 (5)	108 (5)	101 (5)	117 (5)
– $^2P^o_{1/2}$	307.531	355 (3)	948 (4)	872 (3)	103 (4)	440 (3)
– $^2P^o_{3/2}$	311.959	533 (3)	136 (4)	608 (3)	838 (3)	700 (3)
$^4P_{3/2}$ – $^4S^o_{3/2}$	193.759	219 (6)	248 (6)	115 (6)	114 (6)	198 (6)
– $^2D^o_{3/2}$	243.723	233 (4)	190 (4)	777 (3)	110 (4)	186 (4)
– $^2D^o_{5/2}$	245.653	100 (5)	822 (4)	563 (4)	601 (4)	721 (4)
– $^2P^o_{1/2}$	299.098	216 (3)	121 (4)	256 (3)	366 (3)	275 (3)
– $^2P^o_{3/2}$	303.285	907 (3)	400 (4)	120 (4)	168 (4)	958 (3)
$^4P_{5/2}$ – $^4S^o_{3/2}$	189.043	228 (6)	266(6)	*459(4)*	115 (6)	200 (6)
– $^2D^o_{3/2}$	236.304	179 (3)	209 (3)	*174(6)*	129 (3)	152 (3)
– $^2D^o_{5/2}$	238.118	465 (4)	371 (4)	*305(5)*	279 (4)	455 (4)
– $^2P^o_{3/2}$	291.882	116 (2)	.	*612(4)*	970 (1)	570 (1)
$^2P_{1/2}$ – $^4S^o_{3/2}$	188.196	500 (4)	718 (4)	*126(6)*	201 (4)	536 (4)
– $^2D^o_{3/2}$	234.984	290 (6)	230 (6)	*151(3)*	263 (6)	369 (6)
– $^2P^o_{1/2}$	286.043	317 (5)	410 (5)	*250(4)*	686 (5)	550 (5)
– $^2P^o_{3/2}$	289.870	566 (4)	786 (4)	*298(2)*	140 (5)	998 (4)
$^2P_{3/2}$ – $^4S^o_{3/2}$	183.174	366 (4)	498 (4)	225(4)	109 (4)	377 (4)
– $^2D^o_{3/2}$	227.136	170 (3)	104 (4)	780(2)	372 (3)	606 (3)
– $^2D^o_{5/2}$	228.812	263 (6)	207 (6)	163(6)	224 (6)	275 (6)
– $^2P^o_{1/2}$	274.500	153 (5)	179 (5)	151(5)	291 (5)	260 (5)
– $^2P^o_{3/2}$	278.022	500 (5)	717 (5)	441(5)	927 (5)	780 (5)
$^2D_{5/2}$ – $^4S^o_{3/2}$	164.432			218(4)	912 (3)	210 (4)
– $^2D^o_{3/2}$	199.113	367 (5)	312 (5)	220(5)	222 (5)	308 (5)
– $^2D^o_{5/2}$	200.335	263 (6)	282 (6)	144(6)	152 (6)	242 (6)
– $^2P^o_{3/2}$	237.077	333 (5)	334 (5)	253(5)	371 (5)	420 (5)
$^2D_{3/2}$ – $^4S^o_{3/2}$	164.379			387(3)	186 (3)	547 (3)
– $^2D^o_{3/2}$	199.035	260 (6)	333(6)	131(6)	136 (6)	220 (6)
– $^2D^o_{5/2}$	200.255	533 (4)	612 (4)	104(4)	198 (4)	550 (4)
– $^2P^o_{1/2}$	234.402	233 (5)	0.0668	191(5)	288 (5)	353 (5)
– $^2P^o_{3/2}$	236.966	0.14 (2)	0.141	346(5)	483 (5)	595 (5)

Table 4
Absorption oscillator strengths for astrophysically observed As I resonance lines.

Transition					
$4p^25s$-$4p^3$	λ, nm	Present work	[6]	[9] DV	[9] DL
$^4P_{1/2}$ – $^4S^o_{3/2}$	197.262	0.127(15)	0.123(17)	0.06	0.11
$^4P_{3/2}$ – $^4S^o_{3/2}$	193.759	0.059(7)	0.059(8)	0.03	0.06

[9] were taken into the account). Lifetime data are in good agreement between [7] and [9]. One can see, that branching fraction measurements from [9] correlate well with our experimental data sets. Basing on general considerations in our estimation we also took into account the fact that within 3 groups ^4P, ^2P and ^2D – the lifetimes has to be about the same.

From measured branching fractions and selected lifetime data we calculated the transition probabilities for all observed lines, Table 3.

The discrepancy between our data and those from previous experimental studies [6] are caused by different lifetime data used for coupling to the absolute scale. Lifetime data from beam foil experiments [10] were used elsewhere [6]. The differences in measured branching fractions discussed above also impact the data sets for lines 193.7 nm and 307.5 nm.

The most valuable data for application are the absorption oscillator strengths for resonance lines observed in astrophysical objects: results in Table 4 are presented together with data from other studies.

The major part in uncertainties of oscillator strengths in our work are determined by uncertainties in measured lifetime data available from literature [7] (4.5 ± 0.5 ns for $^4P_{1/2}$ state and 4.3 ± 0.5 ns for $^4P_{3/2}$ state).

4. Conclusion

We have measured the branching fractions for As I ($4p^25s$-$4p^3$) transition lines in 180–310 nm spectral range, and obtained the transition probabilities or Einstein coefficients for 26 spectral lines from 7 excited states $4p^25s$ electron configuration, and the absorption oscillator strengths for two arsenic resonance lines observed in astrophysical objects. Our results are in agreement with earlier reported experimental data and theoretical data calculated by the dipole length operator. We compared earlier reported results with our data where smaller uncertainties are present from the use of more appropriate (suitable) experimental setups and calibration data source for the particular aims.

We confirmed previously published values of oscillator strengths and added new values to the data set, thereby supporting published conclusions about the role of arsenic in both the interstellar medium and hot star photospheres.

The main source of errors in arsenic oscillator strengths is uncertainty in the experimental lifetime data. Therefore, in case more accurate lifetime measurements of As I $4p^25s$ states are not made

available, our results will assist more precise determination of oscillator strengths and more accurate concentration values.

Authors statement

We are three authors Uldis Berzins, Arnolds Ubelis, and Armens Bziskjans. U. Berzins is corresponding author and main contributor for this paper. A. Ubelis as senior researcher and took responsibility for conducting the experimental part, and for preparing the arsenic Inductively Coupled Plasma Sources. A Bziskjans PhD student was performing the data collection and his contributed a lot into serving the experimental set up.

Declaration of Competing Interest

The authors declare that they have no known competing financial interests or personal relationships that could have appeared to influence the work reported in this paper.

Acknowledgments

This work was supported by ERDF project No. 1.1.1.5/19/A/003. We also thank Andris Lezdiņš for his contribution in data collection. We are grateful to Prof. Rashid Ganeev for discussions and manuscript revision.

References

[1] Leckrone DS, SeG Johansson, Wahlgren GM. High resolution UV stellar spectroscopy with the HST/GHRS, challenges and opportunities for atomic physics In: HST Workshop: the year of first light. Baltimore: STSCI 1991;83. doi:10.1088/0031-8949/1993/t47/024.

[2] Roederer IU. GermaniumArsenic and Selenium abundances in metal-poor stars. ApJ; 2012;756(36). doi:10.1088/0004-637x/756/1/36.

[3] Roederer IU, Lawler JE. Detection of elements at all three r-process peaks in the metal-poor star HD 160617. Astrophys J 2012;750(76). doi:10.1088/0004-637x/750/1/76.

[4] Roederer IU, Schatz H, Lawler JE, Beers TC, Cowan JJ, Frebel A, Ivans II, Ch Sneden, Sobeck JS. New detections of Arsenic, Selenium, and other heavy elements in two metal-poor stars. Astrophys J 2014;791(32). doi:10.1088/0004-637x/791/1/32.

[5] Cardelli JA. The Abundance of heavy elements in interstellar gas. Science 1994;265:209–13. doi:10.1126/science.265.5169.209.

[6] Lotrian J, Guern Y, Cariou J. Experimentally determined transition probabilities of the system $4p^3$ to $4p^25s$ of neutral arsenic. J Phys B: At Mol Phys 1980;13:685–8. doi:10.1088/0022-3700/13/4/005.

[7] Bengtsson GJ, Berzinsh U, Larsson J, Svanberg S. Determination of radiative lifetimes of neutral Arsenic using time-resolved laser spectroscopy in VUV region. Astron Astrophys 1992;263:440–2.

[8] Lawrence GM. Resonance Transition Probabilities in intermediate coupling for some neutral non-metals. Astrophys J 1967;148:261–8.

[9] Holmgreen L. Theoretically calculated transition probabilities and lifetimes for the first excited configuration np^2 (n+1)s in the neutral As, Sb and Bi atoms. Phys Scr 1975;11:15–22. doi:10.1088/0031-8949/11/1/003.

[10] Anderson T, Jorgenson SW, Sorensen GLJ. Radiative lifetimes in As i and Sb i. J Opt Soc Am 1974;64(891). doi:10.1364/josa.64.000891.

[11] Pehlivan Rhodin A, Hartman H, Nilsson H, Jönsson P. Experimental and theoretical oscillator strengths of Mg I for accurate abundance analysis. Astronomy Astrophys 2017;598(A102):12p.

[12] Ubelis AP, Berzinsh UV. Transition Probability Measurements of Se I Spectral Lines by Emission Method. Phys Scr 1986;34:805–6. doi:10.1088/0031-8949/34/6b/014.

[13] Ubelis AP, Berzinsh UV. Transition probability measurements of Te I spectral lines by methods of emission and absorption of radiation. Phys Scr 1983;28:171–5. doi:10.1088/0031-8949/28/2/005.

[14] Ubelis A, Silinsh J, Berzinsh U, Rachko Z. Vacuum ultraviolet spectra of electrodeless high-frequency lamps. Zhurnal Prikladnoi Spectroskopii 1981;35:216–19. doi:10.1007/bf00605324.

[15] Schiek O, Winter E. Two New Mirror Monochromators. Appl Opt 1965;4(195). doi:10.1364/ao.4.000195.

[16] Berkovskij AG, Gavanin VA, Zaidel IN. Vacuum Photoelectronic Devices. VacuumVacuum 1988;38 55-7. doi:10.1016/0042-207x(88)90269-2.

[17] Mistchenko E.D., Makarov V.A., Shishackaya L.P., Ivanova T.G. Pribori i tehnika eksperimenta, 1977 No. 3, 238 (Russian).

[18] Gladustchak VI, Schreider EYa. Zhurnal Prikladnoi Spectroskopii 1967;6:437 Russian.